Supplemental Material: Resolving the Bethe-Salpeter kernel

Si-Xue Qin[1] and Craig D. Roberts[2,3]

[1] *Department of Physics, Chongqing University, Chongqing 401331, China.*
[2] *School of Physics, Nanjing University, Nanjing, Jiangsu 210093, China*
[3] *Institute for Nonperturbative Physics, Nanjing University, Nanjing, Jiangsu 210093, China*

In this supplement, we provide: details on the derivation of Eqs. (10) from Eqs. (7); illustrative information about the solutions of Eqs. (16), which complete the definition of the Bethe-Salpeter kernel; numerical demonstrations which confirm that our kernel construction preserves both the Gell-Mann–Oakes–Renner relation for meson masses [1, 2] and the quark-level Goldberger-Treiman relation [2, 3], both of which are salient corollaries of DCSB; and describe the BSE solution method that we have employed.

Path from Eqs. (7) to (10).— Using Eqs. (8), Eqs. (7) can be expanded as follows:

$$\begin{aligned}
&[\Sigma_A(k_+) - \Sigma_A(k_-)] + [\Sigma_B(k_+) - \Sigma_B(k_-)] \\
&= \sum_n \int_{dq} K_L^{(n)}[S(q_-) - S(q_+)]K_R^{(n)}\,, \qquad \text{(S.1a)} \\
&- \gamma_5[\Sigma_A(k_+) - \Sigma_A(k_-)] + \gamma_5[\Sigma_B(k_+) + \Sigma_B(k_-)] \\
&= \sum_n \int_{dq} K_L^{(n)}[S(q_+)\gamma_5 + \gamma_5 S(q_-)]K_R^{(n)}\,. \qquad \text{(S.1b)}
\end{aligned}$$

Multiply Eq. (S.1b) from the left with γ_5 and expand the right-hand-sides of both entries in Eqs. (S.1) to obtain:

$$\begin{aligned}
&[\Sigma_A(k_+) - \Sigma_A(k_-)] + [\Sigma_B(k_+) - \Sigma_B(k_-)] \\
&= \sum_n \int_{dq} K_L^{(n)}[\Delta^\pm_{\sigma_A} + \sigma_B(q_-) - \sigma_B(q_+)]K_R^{(n)}\,, \qquad \text{(S.2a)} \\
&- [\Sigma_A(k_+) - \Sigma_A(k_-)] + [\Sigma_B(k_+) + \Sigma_B(k_-)] \\
&= \sum_n \int_{dq} \gamma_5 K_L^{(n)}\gamma_5[\Delta^\pm_{\sigma_A} + \sigma_B(q_-) + \sigma_B(q_+)]K_R^{(n)}\,. \qquad \text{(S.2b)}
\end{aligned}$$

Inserting the decomposition in Eq. (9) into both entries in Eq. (S.2) yields:

$$\begin{aligned}
&[\Sigma_A(k_+) - \Sigma_A(k_-)] + [\Sigma_B(k_+) - \Sigma_B(k_-)] \\
&= \int_{dq} \Big\{ K_{L0}^{(+)}[\Delta^\pm_{\sigma_A} + \sigma_B(q_-) - \sigma_B(q_+)]K_{R0}^{(-)} \\
&\quad + K_{L0}^{(-)}[\Delta^\pm_{\sigma_A} + \sigma_B(q_-) - \sigma_B(q_+)]K_{R0}^{(+)} \\
&\quad + K_{L1}^{(-)}[\sigma_B(q_-) - \sigma_B(q_+)]K_{R1}^{(-)} \\
&\quad + K_{L1}^{(+)}[\sigma_B(q_-) - \sigma_B(q_+)]K_{R1}^{(+)} \\
&\quad + K_{L2}^{(-)}[\Delta^\pm_{\sigma_A}]K_{R2}^{(-)} + K_{L2}^{(+)}[\Delta^\pm_{\sigma_A}]K_{R2}^{(+)} \Big\}\,, \qquad \text{(S.3a)} \\
&-[\Sigma_A(k_+) - \Sigma_A(k_-)] + [\Sigma_B(k_+) + \Sigma_B(k_-)] \\
&= \int_{dq} \Big\{ K_{L0}^{(+)}[\Delta^\pm_{\sigma_A} + \sigma_B(q_-) + \sigma_B(q_+)]K_{R0}^{(-)} \\
&\quad - K_{L0}^{(-)}[\Delta^\pm_{\sigma_A} + \sigma_B(q_-) + \sigma_B(q_+)]K_{R0}^{(+)} \\
&\quad - K_{L1}^{(-)}[\sigma_B(q_-) + \sigma_B(q_+)]K_{R1}^{(-)} \\
&\quad + K_{L1}^{(+)}[\sigma_B(q_-) + \sigma_B(q_+)]K_{R1}^{(+)} \\
&\quad - K_{L2}^{(-)}[\Delta^\pm_{\sigma_A}]K_{R2}^{(-)} + K_{L2}^{(+)}[\Delta^\pm_{\sigma_A}]K_{R2}^{(+)} \Big\}\,, \qquad \text{(S.3b)}
\end{aligned}$$

where we have exploited the notation and characteristics described after Eq. (9) to arrive at these expressions, *viz.* $\otimes_\pm := \frac{1}{2}(\otimes \pm \gamma_5 \otimes \gamma_5)$ and $\gamma_5 K^{(\pm)}\gamma_5 = \pm K^{(\pm)}$.

One can now derive the following relations from appropriate manipulations of Eqs. (S.3):

$$\begin{aligned}
\Sigma_B(k_+) &= \int_{dq} \Big\{ K_{L0}^{(+)}[\Delta^\pm_{\sigma_A} + \sigma_B(q_-)]K_{R0}^{(-)} \\
&\quad + K_{L0}^{(-)}[-\sigma_B(q_+)]K_{R0}^{(+)} + K_{L1}^{(-)}[-\sigma_B(q_+)]K_{R1}^{(-)} \\
&\quad + K_{L1}^{(+)}[\sigma_B(q_-)]K_{R1}^{(+)} + K_{L2}^{(+)}[\Delta^\pm_{\sigma_A}]K_{R2}^{(+)} \Big\}\,, \qquad \text{(S.4a)} \\
&[\Sigma_A(k_+) - \Sigma_A(k_-)] - \Sigma_B(k_-) \\
&= \int_{dq} \Big\{ K_{L0}^{(+)}[-\sigma_B(q_+)]K_{R0}^{(-)} \\
&\quad + K_{L0}^{(-)}[\Delta^\pm_{\sigma_A} + \sigma_B(q_-)]K_{R0}^{(+)} + K_{L1}^{(-)}[\sigma_B(q_-)]K_{R1}^{(-)} \\
&\quad + K_{L1}^{(+)}[-\sigma_B(q_+)]K_{R1}^{(+)} + K_{L2}^{(-)}[\Delta^\pm_{\sigma_A}]K_{R2}^{(-)} \Big\}\,. \qquad \text{(S.4b)}
\end{aligned}$$

At this point, simple combinations of the form

$$\text{term} \pm \gamma_5\,\text{term}\,\gamma_5\,, \qquad \text{(S.5)}$$

where "term" is the left- and right-hand-side of a chosen relation in Eq. (S.4), lead to the following identities:

$$\begin{aligned}
\Sigma_B(k_+) &= \int_{dq} \Big\{ K_{L0}^{(+)}[\Delta^\pm_{\sigma_A}]K_{R0}^{(-)} - K_{L1}^{(-)}[\sigma_B(q_+)]K_{R1}^{(-)} \\
&\quad + K_{L1}^{(+)}[\sigma_B(q_-)]K_{R1}^{(+)} \Big\}\,, \qquad \text{(S.6a)} \\
0 &= \int_{dq} \Big\{ K_{L0}^{(+)}[\sigma_B(q_-)]K_{R0}^{(-)} - K_{L0}^{(-)}[\sigma_B(q_+)]K_{R0}^{(+)} \\
&\quad + K_{L2}^{(+)}[\Delta^\pm_{\sigma_A}]K_{R2}^{(+)} \Big\}\,, \qquad \text{(S.6b)} \\
[\Sigma_A(k_+) - \Sigma_A(k_-)] &= \int_{dq} \Big\{ K_{L0}^{(+)}[-\sigma_B(q_+)]K_{R0}^{(-)}
\end{aligned}$$

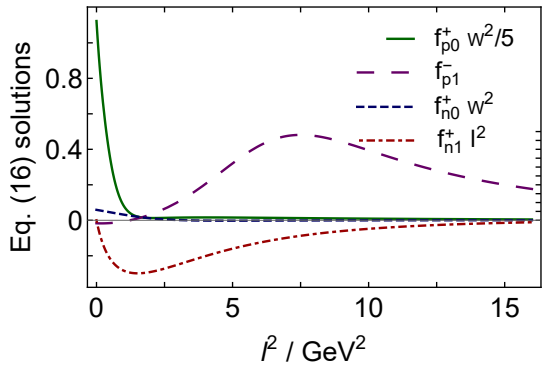

FIG. 1. Scalar functions obtained as solutions of Eqs. (16), which complete the definition of $K_{\rm ad}$ in Eq. (15); hence, $K^{(2)}$. Each curve depicts a dimensionless function. Illustration prepared using $D = (0.72\,{\rm GeV})^2$, $\eta = 1.6$, $m = 3\,{\rm MeV}$, $P^2 = -1\,{\rm GeV}^2$. Rescaling factor $W^2 = \omega^4/[8\pi^2 D] = (0.1\,{\rm GeV})^2$. $W^2 f^{(+)}_{p0}$ is overwhelmingly dominant on a material neighbourhood of $l^2 = 0$, so we divided this function by five in order to present a clear picture.

$$+K^{(-)}_{L0}[\sigma_B(q_-)]K^{(+)}_{R0} + K^{(-)}_{L2}[\Delta^{\pm}_{\sigma_A}]K^{(-)}_{R2}\Big\}\,, \tag{S.6c}$$

$$-\Sigma_B(k_-) = \int_{dq}\Big\{K^{(-)}_{L0}[\Delta^{\pm}_{\sigma_A}]K^{(+)}_{R0} + K^{(-)}_{L1}[\sigma_B(q_-)]K^{(-)}_{R1} + K^{(+)}_{L1}[-\sigma_B(q_+)]K^{(+)}_{R1}\Big\}\,, \tag{S.6d}$$

which are readily recognised as the entries in Eqs. (10). Here, the expression for $\Sigma_B(k_+)$ is related to that for $\Sigma_B(k_-)$ by charge conjugation; hence it contains no additional information and is omitted from the manuscript.

Solving Eqs. (16) and Illustrating their Solutions.— Equations (16) are a pair of complex-valued integral equations, which yield four real-valued linear integral equations whose solutions are the scalar functions that complete $K_{\rm ad}$ and hence $K^{(2)}$. The simplicity of the equations means they may readily be solved by introducing appropriate quadrature rules to replace the integrations and then working with the matrix equations that result.

For illustration and future comparisons, it may be useful to draw examples of the solutions obtained. Using $D = (0.72\,{\rm GeV})^2$, $\eta = 1.6$, $m = 3\,{\rm MeV}$, which produce the most favourable results displayed in Fig. 1, and setting $P^2 = -1\,{\rm GeV}^2$, a value roughly midway between that associated with the ρ and a_1 mesons, one obtains the results drawn in Fig. 1. In preparing this image, we referred to Eqs. (11), (15) and constructed comparisons of rescaled dimensionless functions: since $1/W^2 = 8\pi^2 D/\omega^4$ is the $l^2 = 0$ value of $\mathcal{G}_{\mu\nu}(l)$, it is natural, *e.g.* to compare $W^2 f^{(+)}_{p0}$ with $f^{(-)}_{p1}$.

The f_p functions are associated with that part of the WGT identities which relate to the Dirac scalar piece of the quark propagators, whereas the f_n terms are linked with the vector part. Since DCSB is expressed most strongly in the Dirac scalar part of the propagators, it is therefore unsurprising that the f_p functions are largest.

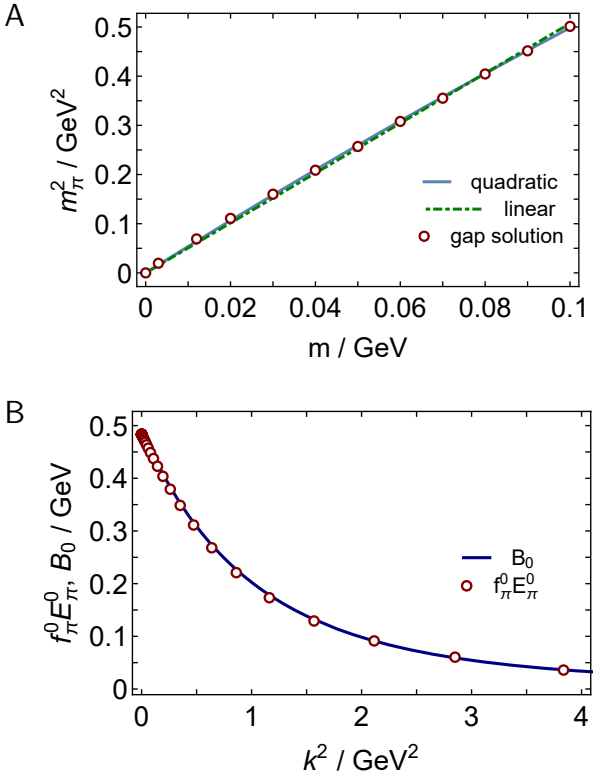

FIG. 2. *Upper panel – A.* Pion mass-squared as a function of current-quark mass, $m_\pi^2(m)$: red circles – numerical solution; solid blue curve – quadratic fit to numerical result, Eq. (S.7a); and dot-dashed green curve – linear fit to result, Eq. (S.7b). *Lower panel – B.* Comparison between the two sides of Eq. (S.9), *viz.* validation of the quark-level Goldberger-Treiman relation. Results in both panels obtained with $D = (0.92\,{\rm GeV})^2$, $\eta = 2/5$.

GMOR and GT Relations.— Using $D = (0.92\,{\rm GeV})^2$, $\eta = 2/5$, we depict $m_\pi^2(m)$ in Fig. 2A. The red circles are the results produced by our Bethe-Salpeter kernel. They are compared with two fits:

$$\text{quadratic}: \quad m_\pi^2 = m \times 5.40(1 - 0.077\, m/m_{\rm m})\,, \tag{S.7a}$$

$$\text{linear}: \quad m_\pi^2 = m \times 5.07\,, \tag{S.7b}$$

where $m_{\rm m} = 0.1\,{\rm GeV}$. There is little to choose between the fits. Thus, the kernel we have constructed preserves the Gell-Mann-Oakes-Renner relation [1, 2].

Furthermore, with a computed value of $f_\pi^0 = 0.093\,{\rm GeV}$, Eqs. (S.7) yield the following results for the $m = 0$ chiral condensate [4]:

$$\text{quadratic}: \quad -\langle\bar{q}q\rangle = (0.286\,{\rm GeV})^3, \tag{S.8a}$$

$$\text{linear}: \quad -\langle\bar{q}q\rangle = (0.280\,{\rm GeV})^3. \tag{S.8b}$$

They are mutually consistent and compare favourably with typical large renormalisation scale values, *e.g.* Refs. [5–7] find $-\langle\bar{q}q\rangle \approx (0.276\,\mathrm{GeV})^3$.

A stringent pointwise test of kernel consistency is provided by the chiral-limit Goldberger-Treiman relation [2, 3]:

$$f_\pi^0 E_\pi^0(k^2; P^2 = 0) = B_0(k^2)\,, \tag{S.9}$$

where the index "0" indicates that the quantity is calculated in the chiral limit and E_π^0 is the dominant (pseudoscalar) term in the pion's canonically normalised Bethe-Salpeter amplitude:

$$\begin{aligned}\Gamma_\pi(k;P) = \gamma_5\,[&iE_\pi(k;P) + \gamma\cdot P F_\pi(k;P)\\ &+\gamma\cdot k G_\pi(k;P) + \sigma_{kP} H_\pi(k;P)]\,.\end{aligned} \tag{S.10}$$

Figure 2B verifies that our kernel delivers solutions that satisfy this identity.

Solving the BSE.— Here we recapitulate a common method for solving the BSE. Namely, the BSE can be written as an eigenvalue problem: $\Gamma_n = \lambda_n(P^2) K\Gamma_n$. Here, $\lambda_n(P^2)$ is the eigenvalue; the Bethe-Salpeter amplitude, Γ_n, is the associated eigenvector; and $\lambda_n(P^2) > \lambda_{n+1}(P^2)$ in the absence of level degeneracies. We use a Euclidean metric, so the on-shell mass for a meson lies at $P^2 < 0$.

The physical solution for the ground-state, $n = 1$, in a given channel is obtained when one finds that timelike value of P^2, closest to $P^2 = 0$, for which $\lambda_0(P^2 = -m_{n=1}^2) = 1$; the first radial excitation is found by locating the value of P^2 for which $\lambda_2(P^2) = 1$; etc. [8, 9].

Since $P^2 < 0$ for all physical systems, the variables $q_\pm$, $k_\pm$ in Eq. (3) are complex valued. The dressed-quark propagator in the kernel is thus sampled on some domain in the complex plane; and we obtain the solution using now well-known algorithms [5, 10]. Those solutions possess complex conjugate poles [5, 11]. With the kernels employed herein, the poles lie outside the sampled domain for meson masses $\lesssim 1.3\,\mathrm{GeV}$. In such cases, the mass and Bethe-Salpeter amplitude are readily obtained.

Today, there are sophisticated methods [12] based on perturbation theory integral representations [13] for handling states with mass $\gtrsim 1.3\,\mathrm{GeV}$. They provide access to the meson mass and Bethe-Salpeter amplitude. However, they are cumbersome to implement. Herein, since we are only interested in masses, we employ the eigenvalue extrapolation procedure introduced in Ref. [14]; to wit, for the heavier systems, we compute $\lambda_n(P^2)$ on a P^2-domain that is unaffected by the propagator poles and then extrapolate in P^2 to locate the zero of $[1 - \lambda_n(P^2)]$. This yields an estimate of the meson's mass along with an uncertainty. It does not provide straightforward access to the associated Bethe-Salpeter amplitude.

In preparing Fig. 1A, eigenvalue extrapolations were used for the b_1', a_1', f_0'. In the first two cases, the uncertainty is smaller than the size of the associated plot marker. In the last case, it is a little larger; so we display a band that expresses the extrapolation uncertainty.

[1] M. Gell-Mann, R. J. Oakes and B. Renner, Phys. Rev. **175**, 2195 (1968).
[2] P. Maris, C. D. Roberts and P. C. Tandy, Phys. Lett. B **420**, 267 (1998).
[3] S.-X. Qin, C. D. Roberts and S. M. Schmidt, Phys. Lett. B **733**, 202 (2014).
[4] S. J. Brodsky, C. D. Roberts, R. Shrock and P. C. Tandy, Phys. Rev. C **82**, 022201(R) (2010).
[5] P. Maris and C. D. Roberts, Phys. Rev. C **56**, 3369 (1997).
[6] P. Maris and P. C. Tandy, Phys. Rev. C **60**, 055214 (1999).
[7] S.-X. Qin, L. Chang, Y.-X. Liu, C. D. Roberts and D. J. Wilson, Phys. Rev. C **84**, 042202(R) (2011).
[8] A. Krassnigg and C. D. Roberts, Fizika B **13**, 143 (2004).
[9] J. Segovia *et al.*, Phys. Rev. Lett. **115**, 171801 (2015).
[10] A. Krassnigg, PoS **CONFINEMENT8**, 075 (2008).
[11] A. Windisch, Phys. Rev. C **95**, 045204 (2017).
[12] L. Chang, I. C. Cloet, C. D. Roberts, S. M. Schmidt and P. C. Tandy, Phys. Rev. Lett. **111**, 141802 (2013).
[13] N. Nakanishi, Prog. Theor. Phys. Suppl. **43**, 1 (1969).
[14] M. R. Frank and C. D. Roberts, Phys. Rev. C **53**, 390 (1996).